Journal of Molecular Structure 921 (2009) 244–250

Contents lists available at ScienceDirect

Journal of Molecular Structure

journal homepage: www.elsevier.com/locate/molstruc

Experimental and *ab initio* structural study of estertin compounds, $X_3SnCH_2CH_2CO_2Me$: Crystal structures of $Cl_3SnCH_2CH_2CO_2Me$ at 120 K and $Br_3SnCH_2CH_2CO_2Me$ at 120 and 291 K

Geraldo M. de Lima [a], Bruce F. Milne [b], Robson P. Pereira [c,d], Ana Maria Rocco [c], Janet M.S. Skakle [e], Anthony J. Travis [f], James L. Wardell [a,*], Solange M.S.V. Wardell [g]

[a] Departamento de Química, ICEx, Universidade Federal de Minas Gerais, 31270-901 Belo Horizonte, MG, Brazil
[b] Centre for Computational Physics, Department of Physics, University of Coimbra, Rua Larga, 3004-516, Coimbra, Portugal
[c] Grupo de Materiais Condutores e Energia, Escola de Química, Universidade Federal do Rio de Janeiro, Centro de Tecnologia, Bloco E, Cidade Universitária, 21945-970, Rio de Janeiro, RJ, Brazil
[d] Grupo de Materiais Condutores e Energia, Rio de Janeiro, Brazil
[e] Department of Chemistry, University of Aberdeen, Meston Walk, Old Aberdeen AB24 3UE, Scotland, UK
[f] The Rowett Research Institute, Greenburn Road, Bucksburn, Aberdeen AB21 9SB, Scotland, UK
[g] FarManguinhos, Fiocruz, Rua Sizenando Nabuco 100, Manguinhos, CEP 21041-250, Rio de Janeiro, RJ, Brazil

ARTICLE INFO

Article history:
Received 28 September 2008
Received in revised form 19 December 2008
Accepted 24 December 2008
Available online 9 January 2009

Keywords:
Chelate complexes
Organotin compounds
Crystallography
Estertin compounds
ab initio calculations

ABSTRACT

The $MeO_2CCH_2CH_2$ ligand in $X_3SnCH_2CH_2CO_2Me$, (X = Cl, Br or I), acts as a *C,O*-chelating group, via the carbonyl group, both in the solid state and in solutions in non-coordinating solvents. The crystal structures of **1** (X = Cl), a redetermination at 120 K and of **I** (X = Br), at 298 and 120 K, are reported. Comparison of the intramolecular Sn—O bond lengths in solid **1** (X = Cl, Br or I) indicates that the strength of the Sn—O interaction increases in the order X = I < Br < Cl. Furthermore, the strength of the Sn—O bond is greater in $Cl_3SnCH_2CH_2CO_2Me$ than in the corresponding ketotin compound, $Cl_3SnCMe_2CH_2COMe$, another chelated complex. Mixtures of **1** (X = Cl) and **1** (X = Br or I) undergo exchange reactions in solution, as shown by NMR spectra, to give all possible halide derivatives, ($Cl_nX_{3-n}SnCH_2CH_2CO_2Me$: n = 0–3: X = Br or I). A series of electronic structure calculations on (**1**: X = F, Cl, Br, I, SCN; R = Me) have been carried out at various levels of theory, including RHF and MP2. Hessian calculations have also been performed on these optimized geometries in order to obtain internal coordinate force constants. Comparisons of the theoretical and experimental structures of **1** (X = Cl, Br and I) are reported.

© 2009 Elsevier B.V. All rights reserved.

1. Introduction

We previously reported an experimental and theoretical study of the structures of the ketotin compounds, $X_3SnCR_2CH_2COMe$ (X = Cl, Br or I) [1]. Ketotin-compounds, $X_3SnCR_2CH_2COR'$ and $X_2Sn(CR_2CH_2COR')_2$, as well as their estertin counterparts, $X_3SnCH_2CH_2CO_2R'$ and $X_2Sn(CH_2CH_2CO_2R')_2$ (X = halide, R = H or alkyl; R′ = alkyl or aryl), are readily available from reactions, first reported in the 1970s [2–6], of $R_2C=CHCOY$ (Y = R′ or OR′), HX and SnX_2 (for $X_3SnCH_2CH_2COY$ compounds) or HX and tin (for $X_2Sn(CH_2CH_2COY)_2$ compounds. Original interest with these compounds was primarily concerned with their industrial potential as precursors of PVC stabilizers [7], but also with regard to their coordination chemistry. Although the potential for use in PVC stabilization has not been realized commercially, the interest in the coordination chemistry, generally of compounds containing $SnCR_2CH_2COY$ moieties, has been maintained over the succeeding decades: of particular interest, has been the coordination modes of the CR_2CH_2COY ligands [1,8,9].

The crystal structures of the estertin halides, $X_3SnCH_2CH_2CO_2R$, (**1**: X = Cl, R = Me [10] at room temperature, (**1**: X = I, R = Me) [11], at 120 K, and (**1**: X = Cl, R = Pr^i) [12] at room temperature, have previously been reported: the geometries around the tin centres in these molecules were generally found to be trigonal bipyramidal, arising from *C,O*-chelation. In non-coordinating solvents, e.g. $CHCl_3$, the Sn—O coordination persists as shown by the ν(CO) values [1670–1650 cm^{-1}] in the IR spectra. NMR spectra also point to tin centers having a higher coordination number than 4.

The crystal structure of (**1**: X = Br, R = Me) has not yet been reported. In order to compare the structures of (**1**: X = Cl, Br and I; R = Me) at the same temperatures, we have obtained the structures of (**1**: X = Cl; R = Me) at 120 K, as well as that of (**1**: X = Br; R = Me) at both 120 and 291 K. Suitable crystals of (**1**: X = F; R = Me) and (**1**: X = SCN; R = Me) could not be obtained. In order to compare experimental and calculated values, a

* Corresponding author. Tel./fax: +55 21 2552 0435.
E-mail address: j.wardell@abdn.ac.uk (J.L. Wardell).

0022-2860/$ - see front matter © 2009 Elsevier B.V. All rights reserved.
doi:10.1016/j.molstruc.2008.12.064

series of *ab initio* geometry optimizations on the structures of (**1**: X = F, Cl, Br, I, SCN; R = Me) were performed at various levels of theory, including the semi-empirical PM3 level and also at the RHF and MP2 levels using the 6-31G(d,p) basis set on H, C, N and O, and the LANL2DZ(d,p) and SBKJC effective-core-potential (ECP) basis sets on F, S, Cl, Br, I and Sn. Internal coordinate (bond) force constants were calculated at the optimized geometries in order to investigate alterations in bond strengths on changing the halogen.

2. Experimental

2.1. General

Melting points were measured using a Kofler hot-stage microscope and are uncorrected. IR spectra were recorded on a Nicolet Magna-IR 760 instrument. NMR spectra were obtained on Bruker 250 MHz and Bruker 400 MHz instruments.

Anhydrous $SnCl_2$ was obtained from the dihydrate on treatment with acetic anhydride under nitrogen, followed by washing with small quantities of anhydrous ether and drying in vacuum. Compounds (**1**: X = Cl; R = Me) [2] and (**1**: X = I; R = Me) [11] were prepared according to published procedures.

2.2. Synthesis

2.2.1. Compound (**1**: X = Cl; R = Me)

M.p. 133–135 °C (lit. value: [10] 132–133 °C).

^{1}H NMR ($CDCl_3$, 250 MHz) δ: 2.24[2H, t, J(H,H) = 7.6 Hz, J($^{119.117}$Sn-^{1}H) = 109,104 Hz, CH_2Sn], 2.94[2H, t, J(H,H) = 7.6 Hz, J($^{119.117}$Sn-^{1}H) = 198,189 Hz, CH_2CO], 3.95[s, 3H, OMe].

^{13}C NMR ($CDCl_3$, 62.5 MHz) δ: 26.1 [J($^{119.117}$Sn-^{13}C) = 840, 800 Hz, CH_2], 29.8[J($^{119.117}$Sn-^{13}C) = 71.3 Hz, CH_2], 56.0[OMe], 138[SCN], 181.8[J($^{119.117}$Sn-^{13}C) = 144 Hz, CO].

^{119}Sn NMR ($CDCl_3$, 93 MHz): δ: −119.7.

IR (KBr′CsI, cm^{-1}), ν: 2994, 2984, 2939, 2912, 2873, 1670(sh) & 1663 (C=O),1475, 1445, 1425, 1410, 1378, 1348, 1266, 1235, 1227, 1157, 1140, 1116, 1037, 1010, 928, 864, 813, 771, 698, 586, 558, 470, 382, 342, 288, 180, 161.

IR (PhMe solution, cm^{-1}): ν: 1679 (CO).

2.2.2. Compound (**1**: X = I; R = Me)

M.p. 64–66 °C (lit. value: [11] 64–66 °C).

IR (KBr/CsI, cm^{-1}), ν: 2987, 2976, 2935, 2923, 2906, 1678(sh) &1661 (C=O), 1475, 1443, 1410, 1382, 1345, 1264, 1222, 1158, 1132, 1036, 1005, 913, 863, 771, 693, 581, 544, 510. 472, 378, 345, 324, 255, 188, 168.

IR (CH_2Cl_2 solution, cm^{-1}), ν: 1679 (CO).

2.2.3. Synthesis of (**1**: X = Br: R = Me)

To a solution of (**1**: X = Cl: R = Me) (3.13 g, 10 mmol) in EtOH (10 ml) was added a suspension of NaBr (8 g) in EtOH (40 ml). After stirring the reaction mixture overnight at room temperature, the mixture was filtered to remove sodium halides. To the filtrate was added a further portion of NaBr (8 g) and EtOH (20 ml) and the mixture stirred once more overnight. The reaction mixture was filtered and the filtrate evaporated to leave a residue. This residue was extracted with $CHCl_3$ and the $CHCl_3$ extracts evaporated. The resulting residue was recrystallized from CH_2Cl_2/hexane.

^{1}H NMR ($CDCl_3$, 250 MHz) δ: 2.38[2H, t, J(H,H) = 7.5 Hz, J($^{119.117}$Sn-^{1}H) = 90 Hz, CH_2Sn], 2.89[2H, t, J(H,H) = 7.5 Hz, J($^{119.117}$Sn-^{1}H) = 195 Hz, CH_2CO], 3.95[s,3H, OMe].

^{13}C NMR ($CDCl_3$, 62.5 MHz) δ: 27.7 [J($^{119.117}$Sn-^{13}C) = 732,700 Hz, CH_2], 28.8[J($^{119.117}$Sn-^{13}C) = 59.6 Hz, CH_2], 55.4[OMe], 138[SCN], 180.3[CO].

^{119}Sn NMR ($CDCl_3$, 93 MHz) δ: −296.

IR (KBr/CsI), ν: 3022, 2997, 2955, 2919, 2864, 1666 (C=O), 1446, 1365, 1270, 1226 (sh), 1184, 1128, 1043, 1010, 954, 897, 857, 751, 693, 584, 464, 437, 386, 317, 246, 228, 211 cm^{-1}.

IR(CH_2Cl_2 solution, cm^{-1}), ν: 1683 (CO) cm^{-1}.

Chem. Anal. Found: C, 11.0; H, 1.8. Calc. for $C_4H_7Br_3O_2Sn$: C, 10.78; H, 1.58%.

2.2.4. Exchange reaction between (**1**: X = Cl) and NaSCN in EtOH

To a solution of (**1**: X = Cl) (3.13 g, 10 mmol) in EtOH (10 ml) was added a suspension of NaSCN (10 g) in EtOH (50 ml). After stirring the reaction mixture overnight at room temperature, the mixture was filtered to remove sodium salts. To the filtrate was added a further portion of NaSCN (10 g) and EtOH (20 ml) and the mixture stirred once more overnight. The reaction mixture was filtered and the filtrate evaporated to leave a residue. This residue was extracted with $CHCl_3$ and the $CHCl_3$ extracts evaporated to leave an oily solid, which liquified on standing. Attempted crystallization from EtOH or $CHCl_3$ produced an amorphous solid.

IR (KBr/CsI), ν: 3008, 2988, 2943, 2909, 2074 & 2053(sh) (SCN), 1655 (C=O), 1561, 1466, 1448, 1409, 1379, 1346, 1263, 1230, 1140, 1099, 1040, 1011, 963, 862, 806, 758, 700, 617, 592, 480, 386, 260, 194 cm^{-1}.

NMR (DMSO-d_6, 250 MHz) δ: 1.38[2H, t, J(H,H) = 7.9 Hz, CH_2Sn], 2.47[2H, t, J(H,H) = 7.9 Hz, CH_2CO], 3.58[s,3H, OMe].

^{13}C NMR (DMSO-d_6, 250 MHz) δ: 25.8 [CH_2], 28.8[CH_2], 51.6[OMe], 137.9[SCN], 173.6[CO].

2.2.5. Compound, **1** (X = Bu)

A mixture of Bu_3SnH (9.00 g, 39.0 mmol), $H_2C{=}CH_2CH_2CO_2Me$ (3.00 g, 30 mmol) and AIBN (0.2 g) was heated at 90 °C for 1 h. After cooling, portions were column chromatographed on SiO_2 with a gradient of CH_2Cl_2/hexane as eluent. The product, $Bu_3SnCH_2CH_2CO_2Me$, was obtained as a thick oil, which was purified by column chromatography on silica using $CHCl_3$: hexane (1:1 v:v) as eluent.

^{1}H NMR ($CDCl_3$, 250 MHz) δ: 0.80–0.85 (6H, m, CH_2Sn of BuSn groups), 0.89 (9H, t, J(H,H) = 8 Hz, CH_3 of Bu groups) 1.00 (2H, m, CH_2Sn of $SnCHCH_2CO_2Me$ group)), 1.26–1.34 (6H, m, CH_2 of Bu groups), 1.40–1.55 (6H, CH_2 of Bu groups], 2.48 [2H, m, CH_2CO], 3.67 [s, 3H, OMe].

IR (KBr/CsI, cm^{-1}), ν: 2956, 2924, 2872, 2853, 1739, 1463, 1436, 1420, 1376, 1355, 1340, 1291, 1203, 1179, 1140, 1122, 1071, 1043, 1021, 1002, 979, 961, 914, 874, 840, 769, 737, 689, 669, 594, 504, 452, 428, 407, 387, 351, 314, 303, 289, 279, 247 cm^{-1}.

Chem. Anal. Found: C, 50.78; H, 9.23. Calc. for $C_{16}H_{34}O_2Sn$: C, 50.95; H, 9.09%.

2.2.6. Compound (**1**: X_3 = Bu_2I)

A mixture of $Bu_3SnCH_2CH_2CO_2Me$, **1** (X = Bu) (3.00 g, 13 mmol), and I_2 (13 mmol) in $CHCl_3$ (30 ml) was maintained at room temperature until complete discoloration had occurred and all volatiles were removed under vacuo to leave an oil. Attempts to distil a portion under vacuum led to decomposition.

^{1}H NMR ($CDCl_3$, 250 MHz) δ: 0.92[6H, t, J(H,H) = 8 Hz , CH_3 of butyl group], 1.3–1.5[8H, m], 1.55–1.70[6H, m], 2.74 [2H, t, J(H,H) = 8 Hz, , J(^{119,117}Sn-^{1}H) = 93, 89 Hz, CH_2CO], 3.78 [s, 3H, OMe].

IR (KBr/CsI, cm^{-1}), ν: 2955, 2922, 2871, 2854, 1689 (C=O), 1571, 1443, 1415, 1357, 1258, 1223, 1184, 1127, 1076, 1028, 961, 878, 743, 679. 601. 521, 408, 366, 237 cm^{-1}.

2.3. Crystallography

Intensity data for (**1**: X = Br) at 291(2) K were collected on a Bruker SMART CCD area detector diffractometer. Data reduction, cell refinement and data collection were achieved using SAINT

software [13] and absorption correction achieved using SADABS [13]. The data for (**1**: X = Cl and Br at 120 K, the data were obtained using the Enraf Nonius KappaCCD area detector diffractometer of the EPSRC National crystallographic service at the University of Southampton, UK. The entire process of data collection, cell refinement and data reduction was accomplished by means of the DENZO [14] and COLLECT [15] programs. Absorption correction was achieved by a semi-empirical method based upon the variation in intensity of equivalent reflections with the program SORTAV [16,17].

The structures were solved by direct methods in SHELXS-97 [18] within the OSCAIL suite of programs [19] and refined in SHELXL-97 [20]. In the final stages of refinement the hydrogen atoms were placed in calculated positions and refined with a riding model. PLATON [21] was used for data analysis. The program ORTEP-3 for Windows was used in the preparation of the Figures. [22]. Crystal data and structure refinement are listed in Table 1.

2.4. Ab initio calculations

All calculations were performed on the SEERAD funded 64-node RRI/BioSS Beowulf cluster at the Rowett Research Institute, Aberdeen, Scotland using GAMESS-US (22 November 2004 R1) [23]. Estertin structures were optimized in the gas phase at the PM3, RHF and MP2 levels of theory. In the *ab initio* calculations the 6-31G(d,p) basis set was used on H, C, N and O, and the LANL2DZ(d,p) or SBKJC effective-core-potential (ECP) basis sets on F, S, Cl, Br, I and Sn. The SBKJC set used was that included with GAMESS-US and the LANL2DZ(d,p) set was obtained from the EMSL Gaussian Basis Set Order Form [24].

Initial calculations at the MP2 level employed the frozen-core approximation; however, it was found that due to the fact that the chemical core electrons were missing on the atoms described by ECP basis sets the GAMESS code was assigning some of the valence orbitals to the frozen (core) region. Because of this the number of frozen core orbitals was set to zero in the MP2 calculations to ensure that all valence electrons in the ECP atoms were included in the correlation treatment.

Following optimization, Hessian calculations were performed on the optimized geometries at the relevant levels of theory in order to obtain the internal coordinate force constants and associated intrinsic vibrational frequencies. The vibrational frequencies obtained were scaled so as to match the C=O stretches in the experimental data since these were the only easily assignable frequencies, yielding a separate scale factor (SF) for each compound at every level of theory used.

Force constants were obtained for **1** (X = F, Cl, Br, I and SCN) by performing a vibrational analysis of the molecules using an internal coordinate system rather than Cartesians. This coordinate system defined the molecule's degrees of freedom in terms of 3N-6 stretches and bends (angles and torsions), making it simpler to assign force constants to particular motions within the molecular force field. For comparative purposes, the force constant for the C—C bond in ethane was calculated at the RHF/6-31G(d,p) level and found to be 4.213×10^{-3} Dyn Å^{-1}.

3. Results and discussion

3.1. Synthesis and spectral studies

The compound, $Br_3SnCH_2CH_2CO_2Me$, **1** (X = Br; R = Me) was prepared by the exchange reaction between excess NaBr and $Cl_3SnCH_2CH_2CO_2Me$, **1** (X = Cl; R = Me)[2] in EtOH. Both the ^{119}Sn

Table 1
Crystal data and structure refinement.

Compound	$Br_3SnCH_2CH_2CO_2Me$	$Br_3SnCH_2CH_2CO_2Me$	$Cl_3SnCH_2CH_2CO_2Me$
Empirical formula	$C_4H_7Br_3O_2Sn$	$C_4H_7Br_3O_2Sn$	$C_3H_4Cl_3O_2Sn$
Formula weight	445.52	445.52	297.10
Temperature (K)	291(2)	120(2)	120(2)
Wavelength (Å)	0.71073	0.71073	0.71073
Crystal system,	Orthorhombic	Orthorhombic	Orthorhombic
Space group	*P* 2(1)2(1)2(1)	*P* 2(1)2(1)2(1)	*P* 2(1)2(1)2(1)
Unit cell dimensions			
a (Å)	9.5220(10)	9.1989(2)	9.1159(2)
b (Å)	10.3843(11)	10.2978(2)	10.1490(3)
c (Å)	10.9527(10)	11.0507(3)	10.4386(3)
Volume (Å3)	1083.00(19)	1046.82(4)	965.75(5)
Z, Calculated density (Mg/m^3)	4, 2.732	4, 2.827	4, 2.043
Absorption coefficient (mm^{-1})	13.380	13.842	3.415
F(000)	808	808	556
Crystal size (mm)	0.35 × 0.26 × 0.24	0.20 × 0.15 × 0.10	0.54 × 0.42 × 0.15
θ range for data collection (°)	2.70–33.00	3.50–27.42	2.97–27.50
Index ranges	−14 <= *h* <= 13	−11 <= *h* <= 11	−10 <= *h* <= 11
	−15 <= *k* <= 7	−13 <= *k* <= 13	−12 <= *k* <= 13
	−16 <=*l* <= 16	−14 <= *l* <= 14	−11 <= *l* <= 13
Reflections collected/unique	10630/4063	2373/2373	6901/2148
	[*R*(int) = 0.0328]	[*R*(int) = 0.0000]	[*R*(int) = 0.0231]
Completeness to 2θ	33.00 99.7%	27.42 99.6%	27.50 0.993%
Absorption correction	Semi-empirical from equivalents	Semi-empirical from equivalents	None
Max. and min. transmission refinement method	0.4231 and 0.2995	0.8081 and 0.2643	
	Full-matrix least-squares on F^2	Full-matrix least-squares on F^2	Full-matrix least-squares on F^2
Data/restraints/parameters	4063/0/92	2373/0/92	2148/0/93
Goodness-of-fit on F^2	0.829	1.084	0.600
Final *R* indices [*I* > 2sigma(*I*)]	*R*1 = 0.0304	*R*1 = 0.0295	*R*1 = 0.0207
	*wR*2 = 0.0643	w*R*2 = 0.0759	w*R*2 = 0.0681
R indices (all data)	*R*1 = 0.0849	*R*1 = 0.0312,	*R*1 = 0.0211
	*wR*2 = 0.0730	*wR*2 = 0.0772	*wR*2 = 0.0691
Absolute structure parameter	0.054(10)	0.061(12)	0.01(3)
Largest diff. peak and hole, e/Å^3	0.606 and −0.790	1.029 and −1.014	1.151 and −1.293
CCDC no.	700793	700794	661484

NMR spectrum in $CDCl_3$ solution and X-ray crystallography indicated that complete exchange had occurred.

Halide exchanges between different compounds (**1:** R = Me) occur readily in solution. Thus mixtures of (**1**: X; R = Me) and (**1**: X′; R = Me) undergo exchanges to give all possible $X_nX'_{3-n}SnCH_2CH_2CO_2R$ compounds (n = integer from 0 to 3) as indicated by ^{119}Sn NMR spectroscopy. Examples of the halide exchanges are: (i) (**1**: X = Cl; R = Me) and (**1**: X = Br: R = Me) in $CHCl_3$ solution produce a mixture of (**1**: $X_3 = Cl_3$; R = Me), (**1**: $X_3 = Cl_2Br$; R = Me), (**1**: $X_3 = ClBr_2$; R = Me) and (**1**: $X_3 = Br_3$; R = Me), having δ^{119}Sn values of −120 ± 2, −171 ± 2, −234 ± 3 and −297 ± 3 ppm, respectively, and (ii) (**1**: X = I; R = Me) and (**1**: X = Cl; R = Me) in $CHCl_3$ solution provide (**1:** $X_3 = Cl_3$; R = Me), (**1**: $X_3 = Cl_2I$; R = Me), (**1**: $X_3 = ClI_2$; R = Me) and (**1:** $X_3 = I_3$; R = Me) having δ^{119}Sn values of −120 ± 2, −340 ± 3, −555 ± 3 and −752 ± 4 ppm, respectively. For the mixed halides, only one chemical shift value was observed, despite the possibilities of isomeric trigonal bipyramidal structures, formed by the different halide groups occupying axial and equatorial positions. Of interest, the two series of δ^{119}Sn values for (**1**: $X_3 = Cl_{3-n}Br_n$; R = Me) and **1** ($X_3 = Cl_{3-n}I_n$; R = Me), show near linear changes with n.

The ^{119}Sn chemical shift values and coupling constants are indicative of the tin centers in (**1;** R = Me) having higher coordination numbers greater than 4 in solution, for example, $J(^{119.117}Sn\text{-}^1H)$ are 90 and 195 Hz for the CH_2Sn and the CH_2CO protons, respectively, in the ^{1}H NMR spectrum of (**1:** X = Br; R = Me).

Tin coordination to the carbonyl oxygen in (**1**: X = Cl, Br or I; R = Me) in non-coordinating solvents, such as chlorocarbons and aromatic hydrocarbons, is also indicated in the IR spectra by ν(CO) values in the range 1660–1675 cm^{-1}. The ν(CO) values for the tetraorganotins, $R_3SnCH_2CH_2CO_2Me$, R = Bu [this study] and R = Ph [25] are 1738 and 1740 cm^{-1}, respectively, and point clearly to a non-coordinated ester group. Tin-oxygen coordination occurs in the mono-iodides, $IR_2SnCH_2CH_2CO_2Me$ (**2**: R = Me or Ph), as shown by the ν(C=O) values *ca.* 1685 cm^{-1} in chlorocarbon solvents: as expected the carbonyl-tin coordination is weaker in the monohalides, **2**, than in the trihalides, (**1**, R = Me), as shown by the ν(C=O) shifts. The ν(Sn—O) values for solid (**1**: R = Me. X = Cl, Br, I or SCN) were observed in the range 377–382 cm^{-1}.

Attempts were made to obtain (**1**: X = F or SCN; R = Me) by exchange reactions between (**1**: X = Cl; R = Me) and NaF or KSCN, in EtOH, in a similar manner as used for (**1**: X = Br; R = Me). While solid products were obtained in each case, neither good elemental analyses nor suitable crystals could be obtained and hence the compositions of these solid products remain unknown. The IR spectra of the products did indicate, in each case, that the carbonyl group was coordinated to tin from the ν(C=O) values at 1640 and 1655 cm^{-1}, for the F and SCN compounds, respectively. Additional IR bands for the F containing compound included those at 547 and 299 cm^{-1} , while additional bands for the SCN-containing compound included those at 2074, 2023, 592.479, 386 and 260 cm^{-1}. The fluoride exchange material was practically insoluble in all organic solvents and attempts to get a more soluble compound on complexation with crown ethers failed. The solubility of (**1**: X = F; R = Me) is markedly distinct from other **1** compounds, including that with X = SCN, and appears to be a polymeric material as most frequently found for organotin fluorides. The isothiocyanato product was particularly sensitive to moisture and heat.

3.2. Solid state studies: X-ray crystallography of (1: X = Br; R = Me) and (1: X = Cl; R = Me)

The crystal structures of (**1**: X = Cl; R = Me at 298 K, [10] and (**1**: X = I, R = Me) at 120 K [11] have been reported, but not that of (**1**: X = Br; R = Me) at any temperature. To allow for comparison of the structures of (**1**: X = Cl, Br and I; R = Me) at similar temperatures, structure determinations of (**1**: X = Cl; R = Me) at 120 K and (**1**: X = Br; R = Me) at 120 K and 291 K have been carried out. The crystals of (**1**: X = Br; R = Me) and (**1**: X = Cl; R = Me) used in the X-ray studies were slowly grown from CH_2Cl_2/hexane solutions. Selected geometric parameters (**1**: X = Br or Cl; R = Me) are listed in Tables 2 and 3. Atom arrangements and numbering schemes for (**1**: X = Br; R = Me) and (**1**: X = Cl; R = Me) are shown in Fig. 1.

The structure determinations of (**1**: X = Cl; R = Me) at 120 K [this study] and at 298 K [10], (**1**: X = Cl, R = Pr^i) [12], (**1**: X = Br, R = Me)] at 120 K [this study] and (**1**: X = I, R = Me) [11] at 100 K, all indicate 5-coordinate tin species in somewhat distorted trigonal bipyramidal arrays arising from intramolecular carbonyl oxygen-tin coordination. The distortion arises in part from the small chelate bite angles. As shown by the torsion angles, the chelate rings in these compounds all have envelope shapes with flaps at the α-carbon atom, C1. The determinations for (**1**: X = Cl or Br, R = Me) indicate no phase change results on changing the temperature: the only differences between the determinations at the different temperatures are the expected larger cell volumes and the flatter chelate rings [Sn—O3—C3—C2—C1] at the higher temperature.

The asymmetric units of both (**1**: X = Br; R = Me) and (**1**: X = Cl; R = Me) consist of single molecules, which are linked via C—H···X (X = Br and Cl) weak intermolecular hydrogen bonds, Figs. 1 and 2. In contrast to the situation in (**1**: X = Br; R = Me) and (**1**: X = Cl; R = Me), two quite distinct independent molecules are found for solid (**1**: X = I; R = Me) [10]. The two independent molecules, A and B, differ appreciably in terms of Sn—O and Sn—I_{axial} bond

Table 2
Selected geometric parameters, °, Å, for X = Br at 120(2) and 291(2) K.

	120(2) K	291(2) K		120(2) K	291(2) K
Sn1—C1	2.142(6)	2.118(5)	C1—Sn1—O32—C3	9.2(4)	2.7(4)
Sn1—O32	2.405(4)	2.415(3)	Sn1—O32—C3—C2	2.2(7)	0.5(6)
Sn1—Br1	2.4557(8)	2.4513(7)	O32—C3—C2—C1	−17.6(9)	−5.1(8)
Sn1—Br2	2.5405(8)	2.5252(8)	C3—C2—C1—Sn1	24.3(7)	7.4(7)
Sn1—Br3	2.4681(8)	2.4577(7)	C2—C1—Sn1—O32	−17.6(5)	−5.3(4)
C3—O32	1.213(7)	1.214(6)			
C1—Sn1—O32	76.2(2)	75.48(19)	C1—Sn1—Br1	131.1(2)	128.94(19)
O32—Sn1—Br1	84.42(11)	84.72(9)	C1—Sn1—Br3	117.4(2)	118.50(19)
O32—Sn1—Br3	84.10(11)	83.75(9)	Br1—Sn1—Br3	104.29(3)	105.09(3)
C1—Sn1—Br2	98.84(18)	99.55(17)	O32—Sn1—Br2	175.08(10)	175.02(9)
Br1—Sn1—Br2	99.26(3)	98.89(3)	Br3—Sn1—Br2	98.06(3)	98.52(3)

Hydrogen bonding parameters at 120(2) K

D—H···A	D—H (Å)	H···A (Å)	D···A (Å)	D—H···A (°)
C2—H2B···Br2^i	0.99	2.88	3.810(7)	157

Symmetry code: i: $-x = 1/2, -y, z + 1$.

Table 3
Selected geometric parameters, Å, °, for $Cl_3SnCH_2CH_2CO_2Me$ at 120(2) K.

Sn1—C1	2.133(4)	Sn1—Cl3	2.3171(10)
Sn1—Cl4	2.3347(9)	Sn1—O32	2.357(3)
Sn1—Cl2	2.3879(10)	O31—C3	1.316(5)
O31—C31	1.450(6)	O32—C3	1.227(5)
C2—C3	1.496(6)	C2—C1	1.515(6)
C1—Sn1—Cl3	132.21(13)	C1—Sn1—Cl4	117.76(13)
Cl3—Sn1—Cl4	103.73(4)	C1—Sn1—O32	77.38(13)
Cl3—Sn1—O32	84.83(8)	Cl4—Sn1—O32	84.06(8)
C1—Sn1—Cl2	99.91(12)	Cl3—Sn1—Cl2	97.90(4)
Cl4—Sn1—Cl2	96.29(4)	O32—Sn1—Cl2	177.06(8)
C3—O31—C31	116.9(3)	C3—O32—Sn1	110.9(3)
C3—C2—C1	113.3(3)	O32—C3—O31	122.9(4)
O32—C3—C2	123.7(4)	O31—C3—C2	113.4(3)
C2—C1—Sn1	112.6(3)		

Hydrogen bonding parameters

D—H···A	D—H (Å)	H···A (Å)	D···A (Å)	D—H···A (°)
C(2)—H(2A)···Cl(2)^{i}	0.99	2.76	3.658(4)	151
C(4)—H(4B)···Cl(4)^{ii}	0.98	2.82	3.777(4)	165

Symmetry codes: i: 1/2 − *x*, 2 − *y*, 1/2 + *z*; ii 1/2 − *x*, 1 − *y*, 1/2 + *z*.

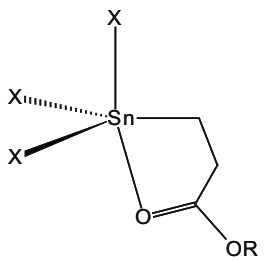

Fig. 1. Compounds **1**.

lengths and O—Sn—C chelate angles, e.g., 2.459(8) Å, 2.7601(10) Å and 76.5(3)° in Mol A, and 2.531(8) Å, 2.188(9) Å and 70.6(3)° in Mol B. Further differences are seen in the hydrogen bonding arrangements involving Mol A and Mol B of (**1**: X = I; R = Me): molecule A acts as an acceptor for two C—H···I hydrogen bonds while molecule B does not act as an acceptor at all [10]. As pointed out by Tiekink and coworkers, [26] intermolecular interactions and crystal packing effects can have significant influences on geometric parameters.

The Sn—O bond lengths at 120 K are 2.347(5) (**1**: X = Cl; R = Me), 2.409(4) (**1**: X = Br; R = Me) and 2.459(8) (Mol. A) and 2.631(8) Å (Mol. B) for (**1**: X = I, R = Me) [10]. These data suggest that the strengths of the Sn—O interactions in **1** follow the increasing electron withdrawing effects of the halogen groups. Furthermore, the strength of the Sn—O bond in $Cl_3SnCH_2CH_2CO_2Me$ is stronger than that in the in the chelated ketotin compound, $Cl_3SnCMe_2CH_2COMe$ [Sn—O = 2.3887(12) Å at 150(2) K and 2.3926(19) Å at 290(2) K] [1].

3.3. Ab initio calculations

Calculated values for selected geometric parameters for (**1**: X = F, Cl, Br, I and SCN; R = Me) are listed in Table 4 for the different levels and/or basis sets used. Comparisons are also made with the experimental values for (**1**: X = Cl, Br and I; R = Me). In all cases the calculations indicated molecular systems even for the (**1**: X = F; R = Me) in the gas phase. However, the solubility of (**1**: X = F; R = Me) strongly suggest a polymeric structure with strong Sn—F intermolecular interactions in both solution and solid phases, as generally found for organotin fluorides. The calculated model is very close to the solid state structures for (**1**: X = Cl and Br; R = Me) and Mol A in (**1**: X = I; R = Me): for these compounds, the C—H···X intermolecular hydrogen bonds, which link molecules in the solid state, are clearly too weak to affect the geometries about tin. for Mol B in (**1**: X = I; R = Me), the C—H···I interactions do have an influence.

The absence of any very strong intermolecular interactions and the presence of a strong intramolecular coordination (C=O···Sn) in these systems, except (**1**: X = F; R = Me) allows the calculation of each molecule as an isolated entity and hence closely representative of the molecular geometry in the solid state found for (**1**: X = Cl; R = Me), (**1**: X = Br; R = Me) and (**1**: X = I; R = Me), especially molecule A. As stated earlier, weak C—H···X intermolecular hydrogen bonding interactions generally link molecules of **1** in the solid state. However for (**1**: X = I; R = Me), the situation is unique in that the two independent molecules are linked alternatively via C—H···I, which impacts on the Sn—O and Sn—I bond lengths within molecule B.

Comparison of the calculated data in Table 4 with the quoted experimental parameters suggests that overall the calculations making use of the 6-31G(d,p):LANL2DZ(d,p) basis set combination provide the best match to experiment. It was found that, contrary to expectation, the MP2 correlation correction did not always lead to an improved fit with the experimental data and in some cases the RHF values were superior in this sense. The PM3 method performed less well in general but in the case of the O—Sn—C angle and the C—C—C—Sn dihedral the semi-empirical PM3 data was found to be in much better agreement with experiment than any of the *ab initio* methods used.

Despite the variations in the quality of the fit between theory and experiment observed, all of the *ab initio* methods used appeared to faithfully reproduce the trends evident in the changes in bond lengths and angles occurring on substitution of different X-ligands. In this respect the PM3 method did not follow the results of the more expensive calculations as is perhaps to be

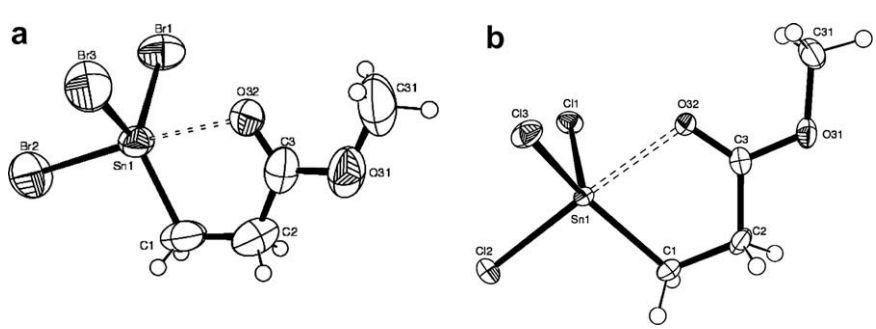

Fig. 2. Atom arrangements and numbering schemes for (a) (**1**: X = Br; R = Me) at 120 K and (b) (**1**: X = Cl; R = Me) at 120 K. Atom arrangements and numbering schemes for (a) (**1**: X = Br; R = Me) at 291 K are similar to those shown for Atom arrangements and numbering schemes for (a) (**1**: X = Br; R = Me) at 120 K.

Table 4
Comparison of selected calculated and experimental geometric parameters for **1**.

Parameter	Ligand	PM3	6-31G(d,p); SBKJC		6-31G(d,p); LANL2DZ(d,p)		X-Ray at	
			RHF	MP2	RHF	MP2	120(2) K	298(2) K
Sn—C	X = F	2.114	2.125	2.135	2.143	2.127		
	X = Cl	2.149	2.136	2.141	2.133	2.137	2.133(4)	2.139(8)
	X = Br	2.144	2.143	2.149	2.140	2.144	2.142(6)	2.118(5)
	X = I	2.169	2.151	2.153	2.149	2.154	2.147(10) Mol A 2.139(12) Mol B	
Sn—X(eq)	X = SCN	2.204	2.144	2.149	2.143	2.148		
	X = F	1.907	1.888	1.930	1.861	1.898		
	X = Cl	2.352	2.370	2.408	2.313	2.316	2.3259(10)	2.310(2)
	X = Br	2.432	2.518	2.560	2.484	2.487	2.4619(8)	2.4545(7)
	X = I	2.677	2.730	2.768	2.699	2.704	2.7601(10) Mol A 2.7188(9) Mol B	
Sn—X(ax)	X = SCN	2.548	2.488	2.456	2.452	2.456		
	X = F	1.910	2.906	1.944	1.839	1.878		
	X = Cl	2.363	2.417	2.443	2.354	2.347	2.3879(10) 2.357(2)	
	X = Br	2.443	2.571	2.601	2.528	2.521	2.5405(8) 2.5252(8)	
	X = I	2.701	2.786	2.815	2.744	2.741	2.7601(10) Mol A 2.7016(9) Mol B	
Sn—O	X = SCN	2.562	2.506	2.477	2.480	2.478		
	X = F	2.529	2.320	2.384	2.345	2.373		
	X = Cl	2.512	2.388	2.424	2.427	2.437	2.357(3) 2.347(5)	
	X = Br	2.398	2.469	2.479	2.516	2.491	2.405(4) 2.415(3)	
	X = I	2.535	2.609	2.562	2.630	2.542	2.459(8) Mol A 2.631(8) Mol B	
C=O	X = SCN	2.615	2.384	2.348	2.345	2.343		
	X = F	1.231	1.211	1.238	1.216	1.239		
	X = Cl	1.233	1.209	1.238	1.207	1.237	1.227(5) 1.23(1)	
	X = Br	1.237	1.206	1.236	1.204	1.235	1.213(7)	1.214(6)
	X = I	1.234	1.202	1.233	1.201	1.234		
	X = SCN	1.232	1.213	1.247	1.216	1.245		
O—Sn—C	X = F	74.97	76.76	76.05	76.10	76.17		
	X = Cl	74.45	75.00	74.81	74.07	74.38	77.38(13)	77.2(3)
	X = Br	76.69	73.30	73.62	72.29	73.21	76.2(2)	75.48(19)
	X = I	73.61	70.67	71.90	70.22	72.17	76.5(3) Mol A 70.6(3) Mol B	
C—C—C—Sn	X = SCN	71.76	75.51	76.64	76.10	76.70		
	X = F	−33.78	−25.38	−32.36	−27.17	−32.58		
	X = Cl	−31.74	−28.78	−34.15	−30.03	−36.31	−16.1(4)	4.6
	X = Br	−24.40	−32.81	−36.52	−34.29	−39.21	24.3(7)	7.4(7)
	X = I	−32.72	−38.48	−39.61	−39.07	−40.95	−1.6(6) Mol A 49.3(11) Mol B	
	X = SCN	−36.91	−30.65	−26.70	−21.82	−31.49		

Table 5
Force constants (MDyn/Å) calculated at each level of theory for (**1**: X = F, Cl, Br, I or SCN; R = Me). Data for angles and torsions were not obtainable from GAMESS-US output. *Note:* for comparative purposes, the force constant for the C—C bond in ethane was calculated at the RHF/6-31G(d,p) level to be 4.213 MDyn/Å.

Parameter	X	PM3	6-31G(d,p); SBKJC		6-31G(d,p); LANL2DZ(d,p)	
			RHF	MP2	RHF	MP2
Sn—C	X = F	1.271	1.885	1.743	3.632	3.168
	X = Cl	1.017	1.778	1.669	1.990	2.028
	X = Br	1.002	1.722	1.621	1.597	1.629
	X = I	0.952	1.669	1.596	1.258	1.258
	X = SCN	0.815	1.722	1.615	1.511	1.480
Sn—X(eq)	X = F	5.108	3.775	3.263	3.978	3.438
	X = Cl	1.523	2.034	1.780	2.276	2.250
	X = Br	1.293	1.715	1.480	1.858	1.824
	X = I	1.608	1.403	1.221	1.480	1.421
	X = SCN	1.424	1.570	1.334	1.680	1.584
Sn—X(ax)	X = F	5.853	3.463	3.070	1.941	1.785
	X = Cl	1.481	1.733	1.594	1.829	1.700
	X = Br	1.318	1.414	1.289	1.771	1.642
	X = I	1.477	1.128	1.033	1.704	1.571
	X = SCN	1.363	1.422	1.249	1.746	1.578
Sn—O	X = F	0.365	0.604	0.563	0.578	0.554
	X = Cl	0.321	0.455	0.482	0.414	0.456
	X = Br	0.192	0.334	0.395	0.318	0.387
	X = I	0.285	0.219	0.301	0.238	0.332
	X = SCN	0.351	0.519	0.505	0.535	0.602
C=O	X = F	12.623	12.185	10.310	12.206	10.227
	X = Cl	12.437	12.291	10.392	12.443	10.353
	X = Br	12.104	12.538	10.431	12.651	10.423
	X = I	12.258	12.901	10.596	12.889	10.483
	X = SCN	12.372	11.903	10.035	11.627	9.802

expected since the minimal-basis description provided by this method is unlikely to be sufficient for the heavier elements involved in many of the compounds studied, such as Br and I. Because of this, it seems inadvisable to use the PM3 approach in future studies of these or related compounds unless higher-level calculations are also performed in order to check the resulting data.

From Table 5, it can be seen that the force constant associated with stretching of the Sn—O bond is reduced and the Sn—O distance is increased as X becomes less electron withdrawing. Lowering of the Sn—O force constant is accompanied by an increase in the C=O stretching force constant and slight decreases in the C=O distance, suggesting that this bond might be absorbing charge density released from the Sn—O region due to decreases in the electron-withdrawing abilities of X. The changes in the Sn—O (decreasing) and C=O (increasing) force constants on going down the ligand series from F to I are complimented by decreases in all of the Sn—X force constants. Thus, it is apparent that the electron-withdrawing power of the ligand is responsible for mediating the changes in the Sn-ester interactions as would be expected from the decreases in electronegativity in the series F > Cl > Br > I.

An interesting result of the calculated geometry and force constant data is that in terms of the Sn—C and Sn—X force constants the SCN ligand appears to be intermediate between Br and I. However, the SCN-containing compound displays the highest force constant for Sn—O and the lowest for C=O which suggests that the Sn atom has much greater electron-accepting ability in this complex. The calculated geometrical data on the other hand seems to place SCN somewhere near F in terms of its effect on the bonds and angles described in Table 4. This is most likely due to the fact that the SCN ligand is much larger and more complex than the others in this study and can therefore interact with the Sn-ester part of the molecule in ways that the halogens cannot such as through non-bonded interactions between the π-systems of the cyano and carbonyl groups. It is clear therefore that despite having been termed a 'pseudohalogen' in terms of its behavior as a ligand in inorganic chemistry the SCN group remains capable of much more complex chemical interactions than the true halogens in similar environments.

Acknowledgements

We are indebted to the EPSRC for the use of both the Chemical Database Service at Daresbury, UK, primarily for access to the Cambridge Structural Database, and the X-ray service at the University of Southampton, UK, for data collection for **2** (X = Cl) at 120 K. We thank CNPq and FAPEMIG Brazil, for financial support. Basis sets were obtained from the Extensible Computational Chemistry Environment Basis Set Database, Version 02/25/04, as developed and distributed by the Molecular Science Computing Facility, Environmental and Molecular Sciences Laboratory which is part of the Pacific Northwest Laboratory, PO Box 999, Richland, WA 99352, USA, and funded by the US Department of Energy. The Pacific Northwest Laboratory is a multi-programme laboratory operated by Battelle Memorial Institute for the US Department of Energy under contract DE-AC06-76RLO 1830. Contact David Feller or Karen Schuchardt for further information.

References

[1] B.F. Milne, R.P. Pereira, A.M. Rocco, J.M.S. Skakle, A.J. Travis, J.L. Wardell, S.M.S.V. Wardell, Appl. Organomet. Chem. 19 (1999) 363.
[2] R.E. Hutton, V. Oakes, Adv. Chem. Ser. 157 (1976) 123.
[3] R.E. Hutton, J.W. Burley, V. Oakes, J. Organomet. Chem. 156 (1978) 369.
[4] J.W. Burley, O. Hope, R.E. Hutton, C.J. Groenenboom, J. Organomet. Chem. 170 (1979) 21.
[5] J.W. Burley, R.E. Hutton, M.R.J. Jolley, C.J. Groenenboom, J. Organomet. Chem. 251 (1983) 189.
[6] J.W. Burley, R.E. Hutton, J. Organomet. Chem. 216 (1982) 165.
[7] D. Lanigen, E.L. Weinberg, Adv. Chem. Ser. 157 (1976) 134.
[8] L.J. Tian, Y.X. Sun, X.J. Liu, G.M. Yang, Z.C. Sheng, Polyhedron 24 (2005) 2027.
[9] L.J. Tian, L.P. Zhang, X.C. Liu, Z.Y. Zhou, Appl. Organomet. Chem. 10 (2005) 198.
[10] P.G. Harrison, T.J. King, M.A. Healey, J. Organomet. Chem. 182 (1979) 17.
[11] R.A. Howie, S.M.S.V. Wardell, Acta Crystallogr. C 58 (2002) m220.
[12] R.A. Howie, E.S. Paterson, J.L. Wardell, J.W. Burley, J. Organomet. Chem. 304 (1986) 301.
[13] Bruker, SADABS, Version 2.03 & SAINT Version 6, Bruker AXS Inc., Madison, WI, USA, 2000.
[14] Z. Otwinowski, W. Minor, Macromolecular Crystallography, Part A, in: C.W. Carter, R.M. Sweet (Eds.), Methods in Enzymology, vol. 276, Academic Press, New York, 1997, pp. 307–326.
[15] R.W.W. Hooft, COLLECT. Nonius BV, Delft, The Netherlands, 1998.
[16] R.H. Blessing, Acta Crystallogr. A 51 (1995) 33.
[17] R.H. Blessing, J. Appl. Crystallogr. 30 (1997) 421.
[18] G.M. Sheldrick, SHELXS-97. Program for the solution of crystal structures, University of Göttingen, Germany, 1997.
[19] P. McArdle, OSCAIL for Windows, National University of Ireland, Galway, Ireland, 2000.
[20] G.M. Sheldrick, SHELXL-97. Program for the crystal structure refinement, University of Göttingen, Germany, 1997.
[21] A.L. Spek, J. Appl. Crystallogr. 36 (2003) 7.
[22] L.J. Farrugia, J. Appl. Crystallogr. 30 (1997) 565.
[23] W. Shmidt, K.K. Baldridge, J.A. Boatz, S.T. Elbert, M.S. Gordon, J.H. Jensen, S. Koseki, N. Matsunaga, K.A. Nguyen, S.J. Su, T.L. Windus, M. Dupuis, J.A. Montgomery, J. Comput. Chem. 14 (1993) 1347.
[24] Available from: <http://www.emsl.pnl.gov/forms/basisform.html>.
[25] P. Harston, R.A. Howie, G.P. McQuillan, J.L. Wardell, E. Zanetti, S.M.S.V. Doidge-Harrison, N.S. Stewart, P.J. Cox, Polyhedron 10 (1991) 1085.
[26] M.A. Buntine, V.J. Hall, F.J. Kosovel, E.R.T. Tiekink, J. Phys. Chem.1 102 (1998) 2472.